Available online at www.sciencedirect.com
SCIENCE DIRECT®
Journal of Solid State Chemistry 177 (2004) 1598–1606
JOURNAL OF SOLID STATE CHEMISTRY
http://elsevier.com/locate/jssc

Site occupancy wave and charge density wave in the modulated structure of $Nd_{0.6}Gd_{0.4}Se_{1.85}$

Thomas Doert,[a,*] Boniface Polequin Fokwa Tsinde,[a] Sven Lidin,[b] and F. Javier García García[b]

[a] *Institute of Inorganic Chemistry, Technical University of Dresden, Mommsenstr. 13, Dresden D-01062, Germany*
[b] *Department of Inorganic Chemistry, Arrhenius Laboratory, Stockholm University, Stockholm S-10691, Sweden*

Received 10 July 2003; received in revised form 4 December 2003; accepted 14 December 2003

Abstract

Single crystals of $Nd_{0.6}Gd_{0.4}Se_{1.85}$ have been prepared by chemical transport reactions starting from pre-annealed powder samples. Satellite reflections observed in X-ray and electron diffraction experiments indicate the presence of a two-dimensional lattice distortion. The origin of this is a site occupancy wave and, coupled to this, a charge density wave in the planar selenium layer of this compound. The modulated structure has been solved and refined from X-ray data using the superspace approach. $Nd_{0.6}Gd_{0.4}Se_{1.85}$ can be described in the (3+2)-dimensional superspace group $P4/n(\alpha\beta\frac{1}{2})\,(\beta-\alpha\frac{1}{2})00$ with lattice parameters of $a = 4.088(1)$ Å, $c = 8.336(1)$ Å. Diffuse scattering contributions have been observed around the satellite reflections which can be understood by the formation of domains with slightly different ordering patterns of Se atoms. Thus, the incommensurate translational parts of the modulation vectors are not constant over the whole crystal and can be described as $\alpha = 0.29 + k$ and $\beta = 0.29 - k$ with $-0.05 \leqslant k \leqslant 0.05$.

Keywords: Modulated structure; Charge density wave; Site occupancy wave; Rare-earth polyselenides; Electron diffraction

1. Introduction

Rare-earth dichalcogenides $LnX_{2-\delta}$ (Ln= Y, La, Ce–Lu; X= S, Se, Te) are both fascinating and puzzling in their crystal chemistry. The common structural feature of all of these compounds (except $EuSe_2$, [1]) is an alternating stacking of puckered $[LnX]$ double slabs and square planar $[X]$ layers, as found in the ZrSSi structure type (space group $P4/nmm$, depicted in Fig. 1). However, no compound without structural distortion or disorder has yet been reported. In most cases, the nature of the distortions can be regarded to be of the Peierls type (e.g., cf. Ref. [2]). Since the rare-earth metals are found in their trivalent state and no $X-X$ bonds are observed in the $[LnX]$ double slabs, charge balancing according to $[Ln^{3+}X^{2-}][X^{-}]$ leads to a formal charge of -1 for the chalcogen atoms of the square layers. This unfavorable electronic situation can be resolved by the formation of X_2^{2-} dimers or other anionic fragments. The clustering of atoms is usually accompanied by a symmetry reduction (e.g., cf. Ref. [3] and references cited therein). For rare-earth diselenides with the composition $LnSe_2$, the square nets always distort to give a herringbone pattern of Se_2^{2-} dimers. These compounds can therefore be described as $[Ln^{3+}Se^{2-}]_2[Se_2^{2-}]$. Only three compounds of this composition, namely $LaSe_2$, $CeSe_2$ and $PrSe_2$, have been structurally characterized to date [4].

In addition to the stoichiometric compounds $LnSe_2$, a number of selenium-deficient compounds $LnX_{2-\delta}$ ($0 < \delta < 0.3$) exist. The compounds $LnSe_{1.9}$ of the lighter rare-earth metals La, Ce, Pr, Nd and Sm crystallize in the $CeSe_{1.9}$ structure type with a 10-fold supercell of the ZrSSi structure [5]. The compounds Ln_8Se_{15} ($LnSe_{1.875}$; $Ln = Y$, Gd, Tb, Dy, Ho, Er) adopt the Gd_8Se_{15} type with a 24-fold supercell of the basic structure [6]. Although some incommensurate superstructures have been reported for $LnSe_{2-\delta}$ compounds [4c,7], only one structure has been solved using the superspace approach. $DySe_{1.84}$ can be described in the (3+2)-dimensional

*Corresponding author. Fax: +49-351-463-37287.
E-mail addresses: thomas.doert@chemie.tu-dresden.de (T. Doert), sven@inorg.su.se (S. Lidin).

0022-4596/$ - see front matter © 2004 Elsevier Inc. All rights reserved.
doi:10.1016/j.jssc.2003.12.013

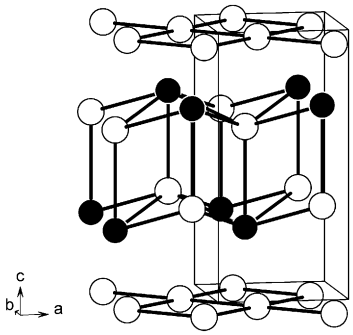

Fig. 1. Substructure of the lanthanide diselenides $LnSe_2$ (ZrSSi type); *Ln* atoms: (●), Se atoms: (○); the unit cell is emphasized.

superspace group $Pm2_1n(\alpha,\beta,\frac{1}{2})$ $(\alpha,-\beta,\frac{1}{2})000$ with $\alpha = 0.33$ and $\beta = 0.27$ [7]. In all cases mentioned above, selenium defects have only been observed in the square layers, while the [*Ln*Se] double slabs remain unaffected. The occurrence of Se deficiencies has, of course, a strong impact on the electronic situation of the [Se] sheet: single Se^{2-} anions and vacant sites occur along with the dimers mentioned above. The arrangement of Se_2^{2-} dimers around the vacancies and single anions has been studied with reference to energetic considerations, and several possible local orientations have been discussed by Lee and Foran [8]. These authors also introduced the term defective lattice charge density waves to characterize the situation in which a crystalline superstructure is produced by an ordered pattern of vacancies.

Since it is somewhat surprising, that at least three different structure types with three slightly different compositions are adopted by the diselenides of trivalent rare-earth metals, we started to investigate ternary compounds containing rare-earth metals that are usually found in different structure types. The first results of these investigations are presented in the following.

2. Experimental section

2.1. Preparation

All preparational steps were carried out under dried Argon (Messer-Griesheim, Krefeld, Germany, 99.96%). Neodymium (Chempur, Karlsruhe, Germany, powder, 99.9%), gadolinium (Chempur, Karlsruhe, Germany, powder, 99.9%) and selenium (Strem, Kehl, Germany, powder, 99.99%) in a molar ratio of 1:1:1.9 were loaded into silica ampoules. The ampoules were sealed under vacuum and placed into an oven where the mixtures were heated to 850°C for 10 days. Single-phase, gray microcrystalline samples were obtained, as judged by their X-ray powder diagrams. Single crystals were prepared by chemical transport reactions starting from the pre-reacted samples over a temperature gradient from 850°C to 800°C with iodine (about $3\,g\,cm^{-3}$) as transport agent. After 10 days, shiny, gray metallic platelets up to 0.15 mm were found at the cold ends of the ampoules.

2.2. Composition

EDX analyses (Zeiss Digital Scanning Microscope 982 Gemini with a Noram Voyager analytic unit) were performed on freshly cleaved faces of several crystals. The overall composition $Nd_{0.60(2)}Gd_{0.40(2)}Se_{1.90(3)}$ was determined; no traces of any other element were found. Refinement of the occupancies of the metal atoms during refinement of the average structure yielded values of 0.64(8) and 0.36(8), respectively. Due to large correlations with some modulation parameters, the occupancies were fixed at 0.6 for Nd and 0.4 for Gd during the refinement of the modulated structure. Refinement of the occupancies of the layer atom Se(2) yielded 0.85(1) for the modulated and 0.86(1) for the average structure, respectively. These refined occupancies are slightly smaller than the result of the EDX analyses, but since both calculations yielded the same value within standard deviation, we refer to the compound as $Nd_{0.6}Gd_{0.4}Se_{1.85}$.

2.3. HRTEM and electron diffraction

Samples for HRTEM and electron diffraction were prepared by grinding single crystals under *n*-butanol. A few drops of this suspension were placed onto a carbon-coated copper grid, and the alcohol was allowed to evaporate.

Electron diffraction studies were carried out with a JEOL JEM-2000 FX electron microscope, operated at 200 kV. For HRTEM investigations a JEOL JEM-3010 electron microscope, operated at 300 kV, was used.

2.4. X-ray investigations

Crystals of the title compound were mounted on quartz fibers, and precession records were taken. Satellite reflections were found on precession records $h\,k\,0.5$ and $h\,k\,1.5$, indicating a two-dimensional incommensurate modulation of the structure with the rational component of the modulation vectors being $\frac{1}{2}$ along c^*. Subsequent recording of a complete data set of main reflections, first-order satellites, and cross-terms was carried out on a STOE IPDS diffractometer with monochromatized Mo$K\alpha$ radiation. The modulation vectors were determined using the STOE IPDS software package [9]. Absorption correction of the (3 + 2)-dimensional data set was performed using the JANA2000 software package [10]; the shape of the crystal was taken from the corresponding fit on the average structure [11]. Structure refinements were

carried out with JANA2000 against F^2. Representations of the crystal structure were prepared with the program DIAMOND [12].

3. Results and discussion

3.1. Structure determination and refinement

The X-ray diffraction pattern suggests Laue class $4/mmm$ and the reflection condition $h\,k\,0 : h + k = 2n$ for the main reflections indicates the space group $P4/nmm$ for the basic structure. Since no additional extinction conditions for the satellites were observed, the $(3+2)d$ superspace group $P4/nmm(\alpha\alpha\frac{1}{2})\,(\alpha - \alpha\frac{1}{2})00mm$ with $\alpha = 0.29$ is unambiguously defined [13].[1] However, some of the satellites showed streaking perpendicular to the direction of the modulation vector.

HRTEM images recorded along [001] exhibit a multi-domain structure for the investigated crystals. From the distribution of dark and bright spots in the image, the lattice parameters of $a = b \approx 4.1$ Å can be extracted. Fig. 2a shows an electron diffraction image of a crystal of $Nd_{0.6}Gd_{0.4}Se_{1.85}$ recorded along [001] (left; all crystallographic directions are given with respect to the basic structure) and a schematic illustration of an enlarged section around one main reflection (right). First-order satellites related to the modulation vectors q_1 and q_2 cannot be found in this zone due to the contribution of $\frac{1}{2}$ along c^*. Instead, second-order satellites according to $2q_1$ and $2q_1$ (some are indicated by black arrows in the figure) and cross-terms according to $q_1 + q_2$ and $q_1 - q_2$ (some emphasized by gray arrows) occur. All satellites show intensity maxima well defined by q_1 and q_2, but extensive streaking is observed perpendicular to the respective modulation direction for the second-order satellites as well as along [110] and $[1\bar{1}0]$ simultaneously for the cross-terms. All main reflections, on the contrary, are sharp and distinct spots. Fig. 2b shows a SAED pattern taken along $[1\bar{1}0]$ with the reciprocal lattice vectors indicated. The contribution of the modulation vector along c^* can clearly be seen. Satellites up to the order of at least four are observed

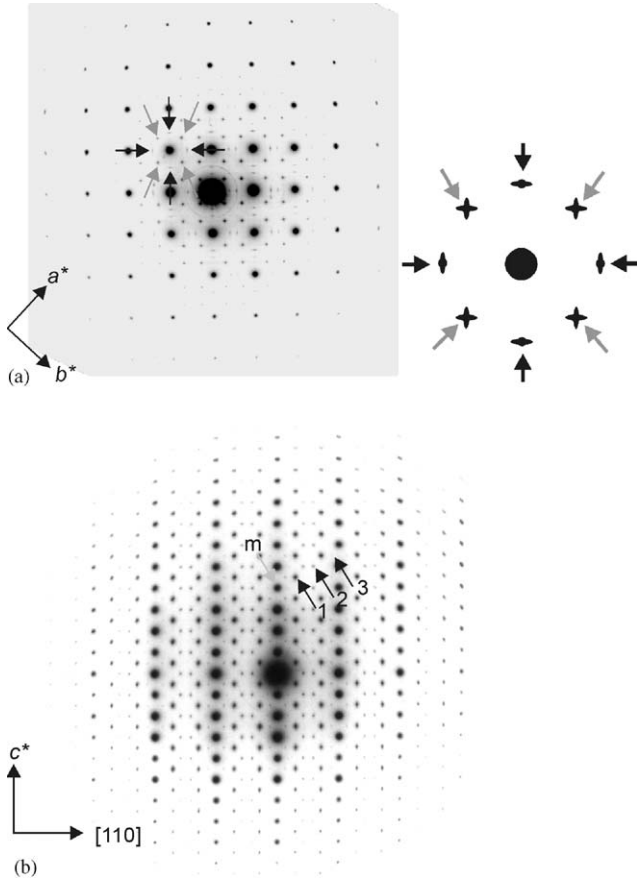

Fig. 2. (a) Left: SAED pattern taken along [001], satellites are indicated by arrows, right: schematic illustration representing the intensity distribution of second-order satellites (black arrows) and cross-terms (gray arrows) around one main reflection. (b) SAED pattern taken along $[1\bar{1}0]$, three satellites and one main reflection are indicated by arrows.

and no streaking of reflections is found in this direction. A set of satellites of order 1, 2, and 3, and the respective main reflection is indicated by arrows.

If we consider the intensity maxima of all reflections only, the whole diffraction pattern again resembles $4/mmm$ symmetry. The modulation vectors are then $q_1 = (\alpha, \alpha, \frac{1}{2})$ and $q_2 = (\alpha, -\alpha, \frac{1}{2})$ with $\alpha = 0.29$. The streaks of the satellites in the $h\,k\,0$ plane, clearly contradicting the $4/mmm$ symmetry, indicate a disturbance of the long-range order perpendicular to the layer. Since the diffuse scattering is only observed near satellite reflections, the disorder must be coupled to that part of the structure which is principally affected by the lattice distortion. This is, as we will see, the defective [Se] layer. The [Se] sheet consists of a few building units which can be arranged in different ways. Since we are dealing with a layered-type structure (Fig. 1), information transfer between the [Se] sheets can be neglected. We can thus assume that the crystal consists of different domains with different ordering patterns. In the superspace approach, we cover this by considering slightly different

[1] During X-ray investigations of several crystals, we found values between 0.289 and 0.292 for the translational parts α and β of the modulation vectors. These values are slightly larger, but still close to the commensurate value of 2/7. The structure can thus also be refined in a commensurate $7a \times 7b \times 2c$ supercell (space group $P4/n$). This structure refinement converged to residuals of $R_1 = 0.042$, $wR_2 = 0.127$ for 9394 data and 429 parameters. All Se atoms could only be refined isotropically; the standard deviations of the atomic parameters are at least twice as large as for the superspace refinement, those of the interatomic distances are about 10 times larger. The structure model gave no resolution of the disordered Se layer. Considering this, we prefer the superspace approach for this problem, especially when we take the reduced number of parameters in the modulated refinement and the low intensities of the satellites reflections into account.

modulation vectors $q'_1 = (\alpha + k, \alpha - k, \frac{1}{2})$ and $q'_1 = (\alpha - k, -(\alpha + k), \frac{1}{2})$ with $k =$ const. for each domain; different domains can have different values of k. As a result, k runs from $-\delta$ to $+\delta$ for the whole crystal and streaking perpendicular to the modulation direction will occur for all satellites of the type nq_1 and nq_2 ($n = 1, 2, 3, \ldots$). For the cross-terms $q'_1 + q'_2$ and $q'_1 - q'_2$, the resulting scattering vectors are $(2\alpha, -2k, 0)$ and $(2k, 2\alpha, 0)$, respectively, explaining the simultaneous streaking along both modulation directions. The observed diffraction pattern, a superposition of the contribution of all domains, can be described with Laue symmetry $4/m$. In accordance with these considerations, the modulation vectors $q'_1 = (\alpha, \beta, \frac{1}{2})$ and $q'_2 = (\beta, -\alpha, \frac{1}{2})$ with $\alpha = \beta = 0.29$ were defined, and the structure of $Nd_{0.6}Gd_{0.4}Se_{1.85}$ was solved and refined in superspace group $P4/n(\alpha\beta\frac{1}{2})$ $(\beta - \alpha\frac{1}{2})00$ (s. below). Since the intensity of the streaks is comparatively weak and the observed intensity maxima for all satellites are compatible with $4/mmm$ symmetry, we can assume that one high symmetric phase predominates, which can be described in superspace group $P4/nmm(\alpha\alpha\frac{1}{2})$ $(\alpha - \alpha\frac{1}{2})00mm$.

Note, that an equivalent explanation for the streaking exists if we consider modulation vectors of the kind $q_0 = (\alpha, \beta, \frac{1}{2})$ and $q'_0 = (\alpha, -\beta, \frac{1}{2})$ with $\alpha \approx \beta$. These vectors are compatible with orthorhombic symmetry at most. An orthorhombic superstructure with these modulation vectors and $\alpha = 0.27$ and $\beta = 0.33$ has been found for $DySe_{1.84}$ [7].

In order to lose the commensurate part of the modulation vectors, the c-axis of the unit cell of the average structure was doubled and the superspace centering condition $(00\frac{1}{2}\frac{1}{2}\frac{1}{2})$ was introduced. Taking the transformed atomic parameters of the ZrSSi type, a conventional 3D starting model was readily available and could be refined to residuals of $R_1 = 0.027$ and $wR_2 = 0.074$ for all main reflections. Se(2), the selenium atom of the square layer showed large pancake-shaped displacement parameters indicating the directions of the modulation.

In a next step, first-order harmonics for the positional displacements of all atoms were introduced but the refinement did not yield a satisfactory structure model ($wR_2 \approx 0.36$ for all first-order satellites). From the resulting Fourier map, depicted in Fig. 3, it is apparent that the atom Se(2) partly follows a sawtooth-like modulation. Such discontinuous behavior is quite well known and can be fitted fairly suitably in four dimensions. However, a sawtooth function in five dimensions is not available in any refinement software, and the use of a crenel function for the fit of the occupation modulation was excluded for the same reason. Instead, a harmonic function with first-order coefficients for the positional modulation of the *Ln* and Se(1) atoms and first- and second-order coefficients for the occupancy and positional modulation of Se(2) was chosen. This refinement resulted in a satisfactory structure model with reasonable interatomic distances. In the final stages of the refinement, modulation waves for the displacement parameters of all atoms were also introduced. It should be noted that a fit of any discontinuous behavior with a harmonic function can only result in an approximation and may show some over- and undershooting as well as notable truncation effects.

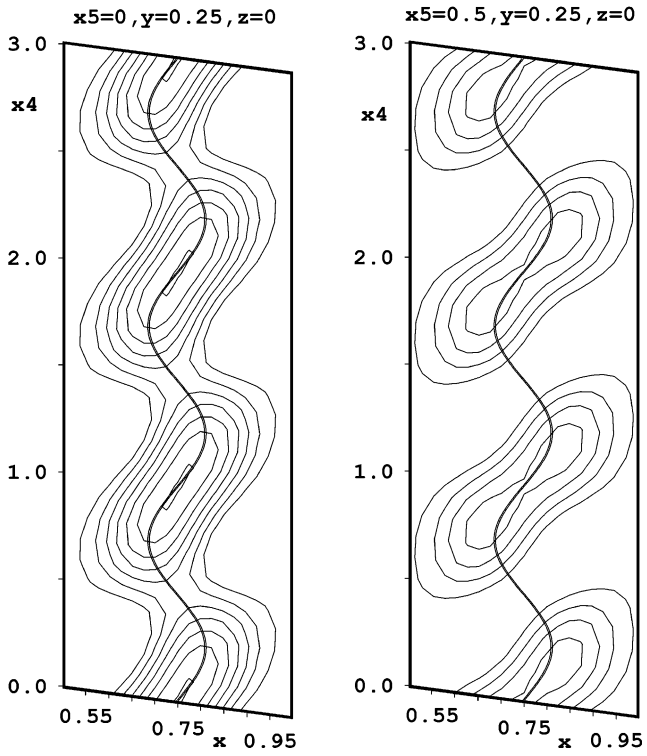

Fig. 3. Sections of a Fourier map in $(3+2)d$ space along one modulation direction calculated around atom Se(2) which is indicated by the central line; x4 and x5 are the external basis vectors corresponding to q'_1 and q'_2, respectively (cf. Ref. [14], for a definition of x4 and x5); the discontinuous nature of the modulation can clearly be seen.

Since the high Laue symmetry of the diffraction pattern could be induced by twinning, this option was tested but the introduction of the corresponding twin law yielded no improvement. Transformation of the structure model to orthorhombic and monoclinic superspace groups and subsequent refinements gave no improvements either. All structure models calculated in different space groups were very much alike; some could be excluded by the occurrence of short Se–Se contacts ($\leqslant 2.2$ Å). We take this as a strong indication that the choice of the superspace group $P4/n(\alpha\beta\frac{1}{2})$ $(\beta - \alpha\frac{1}{2})00$ does not lead to general misrepresentations in the structure description. The bad residual values for the second-order satellites, which are all cross-terms ($h\,k\,l\,m : m$ and $n = \pm 1$) in this case, are caused

Table 1
Crystallographic data for $Nd_{0.6}Gd_{0.4}Se_{1.85}$

Formula; formula weight; $F(000)$	$Nd_{0.6}Gd_{0.4}Se_{1.85}$; 296.3 g mol^{-1}; 498
Crystal size	$0.03 \times 0.03 \times 0.05$ mm^3
Diffractometer	STOE IPDS, graphite monochromator, Mo$K\alpha$
Reflections	$-5 \leqslant h, k \leqslant 5$; $-21 \leqslant l \leqslant 21$; $-1 \leqslant m, n \leqslant 1$
	$2.3° < \theta < 26.8°$; 14301 refl. collected
Main reflections and satellites	1338 independent, 680 obs. with $I > 3\sigma(I)$
Main reflections only	149 independent, 145 obs. with $I > 3\sigma(I)$
First-order satellites	596 independent, 405 obs. with $I > 3\sigma(I)$
Second-order satellites	593 independent, 130 obs. with $I > 3\sigma(I)$
R_{int}; R_{sigma}	0.130; 0.017
Superspace group; Z	$P4/n(\alpha\beta\frac{1}{2})\,(\beta - \alpha\frac{1}{2})00$ (No. 2593); 4
Lattice parameters	$a = 4.088(1)$ Å
	$c = 16.672(3)$ Å
	$V = 278.6(1)$ Å^3
Centering vector	$(0, 0, \frac{1}{2}, \frac{1}{2}, \frac{1}{2})$
Modulation vectors	$q'_1 = (\alpha, \beta, \frac{1}{2})$, $q'_2 = (\beta, -\alpha, \frac{1}{2})$; $\alpha = 0.29 + k$,
	$\beta = 0.29 - k$; $-0.05 \leqslant k \leqslant 0.05$ (estimated)
Calc. density; abs. coefficient	7.06 g cm^{-3}; 44.63 mm^{-1}
Abs. correction	Analytical [10,11], $T_{min} = 0.03$, $T_{max} = 0.11$
Refinement	JANA2000, full matrix against F^2 [10]
	43 parameters
Weighting scheme	$w = 1/[\sigma^2(I) + (0.00032(I^2)]$
Residual values	
Main reflections and satellites:	
R_1, w$R_2(I > 3\sigma)$; R_1, wR_2(all I)	0.053, 0.101; 0.129, 0.125
Main reflections only:	
R_1, w$R_2(I > 3\sigma)$; R_1, wR_2(all I)	0.031, 0.079; 0.032, 0.079
First-order satellites only:	
R_1, w$R_2(I > 3\sigma)$; R_1, wR_2(all I)	0.056, 0.104; 0.089, 0.106
Second-order satellites (cross-terms):	
R_1, w$R_2(I > 3\sigma)$; R_1, wR_2(all I)	0.235, 0.435; 0.639, 0.791
GooF ($I > 3\sigma$; all I)	2.78, 3.20
Largest diff. peak/hole	$+2.1/-2.3$e Å^{-3}

by the very low intensity and poor statistics for these reflections: only about 30% have intensities above $3\sigma(I)$, and less than 50% above $1\sigma(I)$. In the $F_o - F_c$ table, the deviations for the cross-terms are not larger than for other reflections. Nevertheless, these reflections are important for the refinement and stabilization of the structure model.

The final structure model for $Nd_{0.6}Gd_{0.4}Se_{1.85}$ and the results of the refinements are stated in Tables 1–3 (crystallographic information, atomic parameters and Fourier coefficients of the modulation waves, respectively); selected interatomic distances are given in Table 4.[2]

3.2. Structure description and discussion

As stated above, the modulation mainly affects the Se(2) atom of $Nd_{0.6}Gd_{0.4}Se_{1.85}$ (cf. Table 3). On the one hand, distinct vacancies occur as a result of the occupancy modulation of this atom. The positional modulation, on the other hand, leads to the rearrangement of the remaining Se atoms to form discrete anionic entities. The resulting [Se] layer is illustrated in Fig. 4. The section covers seven times the basic lattice parameters a and b and thus more than one modulation period along q'_1 and q'_2 each. A relatively high cutoff value of 0.65 for the modulated site occupancy factors (s.o.f.) has been chosen in order to represent the composition of the selenium layer best.

Besides the obvious occurrence of distinct vacancies, the Se(2)–Se(2) distances vary from 2.44 to 3.45 Å in the modulated phase and fall in three groups: a first group

Table 2
Atomic coordinates, occupancies and displacement parameters U (Å$^2 \times 10^4$)

Atom	Occ.	x	y	z	$U_{11} = U_{22}$	U_{33}
Nd(1)	0.6	1/4	1/4	0.6368(1)	96(3)	150(4)
Gd(1)	0.4	1/4	1/4	0.6368	96	150
Se(1)	1.0	1/4	1/4	0.8168(1)	94(4)	112(4)
Se(2)	0.85(1)	1/4	1/4	0	295(9)	99(8)

[2] Further details on the crystal structure investigation can be obtained from the Fachinformationzentrum Karlsruhe, D-76344 Eggenstein-Leopoldshafen (fax: (++49)7247-808-666; e-mail: crysdata@fiz.karlsruhe.de), on quoting the depository number CSD 413247.

Table 3
Fourier coefficients of the site modulation (S_{sn}, C_{sn}) and the occupancy modulation (C_{on}) waves (S= sin, C= cos term, the subscripts 1 and 2 refer to modulation waves q'_1 and q'_2, subscripts 3 and 4 to $q'_1+q'_2$ and $q'_1-q'_2$, resp.)

Atom	$S_{x1}=-S_{y2}$	$S_{y1}=S_{x2}$	$S_{x3}=-S_{y4}$	$S_{y3}=S_{x4}$	$C_{z1}=C_{z2}$	$C_{o1}=C_{o2}$	$C_{o1}=C_{o2}$
Nd(1)	−0.0045(2)	−0.0046(2)	—	—	0.0060(1)	—	—
Gd(1)	−0.0045	−0.0046	—	—	0.0060	—	—
Se(1)	0.0030(2)	−0.0032(2)	—	—	0.0038(1)	—	—
Se(2)	0.0478(5)	−0.0479(5)	−0.0140(7)	−0.0002(8)	0.0001(1)	0.166(8)	−0.040(9)

Table 4
Selected interatomic distances (Å)

	Ave.	Min.	Max.	Δ	
M–Se(1)	2.995(1)	2.928(2)	3.072(2)	0.144	1×
M–Se(1)	2.990(1)	2.939(1)	3.053(1)	0.114	4×
M–Se(2)	3.065(4)	3.061(4)	3.260(4)	0.199	4×
Se(2)–Se(2)	2.941(8)	2.346(7)	3.455(7)	1.109	4×

with short distances between 2.44 and 2.64 Å (depicted as continuous lines in Fig. 4, left and right), a second group with distances from 2.70 to 2.92 Å (dashed lines in Fig. 4, right), and a third with distances >3.00 Å (not emphasized in Fig. 4). If only the short contacts (<2.64 Å) are taken into account, the selenium sheet can be described as containing dimers, bent trimers and a number of monomeric anions, some of the latter arranged in groups (Fig. 4, left). If we also consider Se–Se distances between 2.70 and 2.92 Å, the image of the [Se] layer now shows eight membered rings and fragments of these eight rings around the vacancies with chains of linear trimeric anions and Se^{2-} anions running between them (Fig. 4, right). Similar eight rings consisting of a pinwheel-like arrangement of four Se_2^{2-} dumbbells are found in the selenium layers of the compounds of the $CeSe_{1.9}$ type (Fig. 5, left, e.g., $NdSe_{1.9}$ [5b]). In the structures of Gd_8Se_{15} (Fig. 5, right, [6f]) and $DySe_{1.84}$ ([7], not depicted) eight rings consisting of a disordered arrangement of dimers occur. In the structures of $YSe_{1.85}$, $HoSe_{1.875}$, $DySe_{1.875}$ and $ErSe_{1.85}$, as well as in those of the related sulfides $DyS_{1.76}$, $DyS_{1.84}$, and $HoS_{1.86}$, defect chalcogen eight rings were found [15]. It is thus not surprising to find a similar kind of selenium fragments in $Nd_{0.6}Gd_{0.4}Se_{1.85}$ Since we are dealing with a partially disordered structure, the eight rings and eight-ring fragments are likely to consist of a disordered pattern of dumbbells, or dumbbells and single Se^{2-} anions, respectively.

The bent trimers in the present structure exhibit bond angles between 87° and 89°, in contrast to the bond angle of approximately 104° found in the bent Se_3^{2-} entities of the alkali metal selenides A_2Se_3 (A= K, Rb, Cs, e.g., Ref. [16]) Whether this is due to crystal packing effects or whether the trimers appear as a result of disorder cannot be deduced from our data.

Besides this positional disorder another feature should be noted. Some chalcogen positions of the eight rings of $YSe_{1.85}$, $HoSe_{1.875}$, $DySe_{1.875}$, $ErSe_{1.85}$, and the eight-ring fragments of $DyS_{1.76}$, $DyS_{1.84}$, and $HoS_{1.86}$ are not fully occupied [6f,15]. In $Nd_{0.6}Gd_{0.4}Se_{1.85}$, one of the Se positions in most of the eight-ring fragments has an occupation factor between 0.65 and 0.7, i.e., slightly above the threshold for representation in Fig. 4. The linear chains between the eight rings are almost not affected by the occupancy modulation; all atoms have s.o.f. close to 1.0. The linear trimers within these chains may also be composed of a disordered sequence of Se^{2-} monomers and Se_2^{2-} dimers; the occurrence of Se_3^{4-} anions is somewhat unlikely since these entities have never been observed in the solid state. The Se–Se distances of the linear trimers are similar to those found in the eight rings (2.59–2.90 Å). In the [Se] layers of the respective binary selenides, the shortest Se–Se distances were found to be 2.48 Å for the Se_2^{2-} dimers and 2.92 Å between two dimers in $NdSe_{1.9}$; 2.41/2.49 Å for the ordered and 2.50/2.51 Å for the disordered dumbbells in the eight ring, and 2.75/2.78 Å between two disordered dimers in Gd_8Se_{15} [5b,6f]. The shortest contact between dimers and single anions is 3.17 Å in $NdSe_{1.9}$ but only 2.94 Å in Gd_8Se_{15}.

As has been pointed out by Lee and Foran [8], the radial or spoke-like arrangement of four Se_2^{2-} dimers around a single Se^{2-} anion and the eight-ring or pinwheel-like arrangement of dimers around vacancies are the most favorable structural patterns for defective selenide layers. The same surely holds for defective sulfide layers [15], but not necessarily for telluride sheets, in which several different Te entities can be found [17]. The only structure, in which a fully ordered spoke-like pattern in the defective square layers occurs are those of the $CeSe_{1.9}$ type. All other structures contain disordered layers; however, as is visible from Fig. 4, the tendency to adopt this favorite orientation is widely conserved.

During the solution of the modulated structure of $DySe_{1.84}$, several models were developed and refined to similar residuals. Since no decision about the crystallographically correct model was possible from the diffraction data, the second moment scaled Hückel method based on idealized starting models was used [7,18]. The models found to be lowest in energy

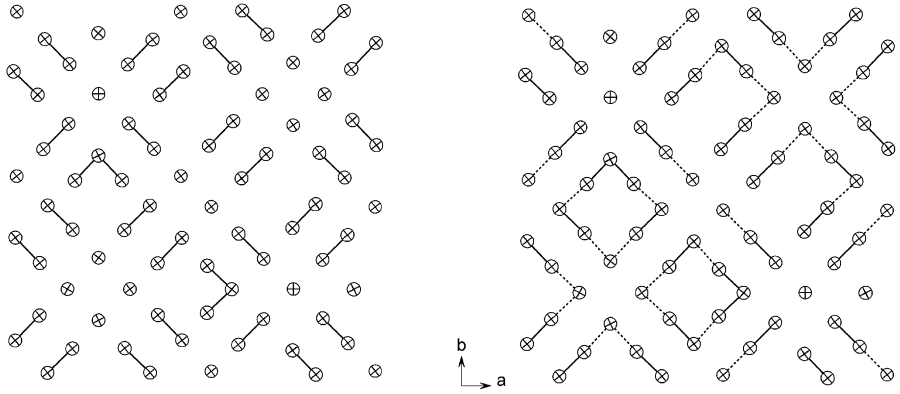

Fig. 4. Se-deficient [Se]-sheet of $Nd_{0.6}Gd_{0.4}Se_{1.85}$, distances between 2.33 and 2.66 Å depicted as continuous lines (left and right), distances from 2.70 to 2.91 Å as (- - -) (right), thermal ellipsoids with 99% probability.

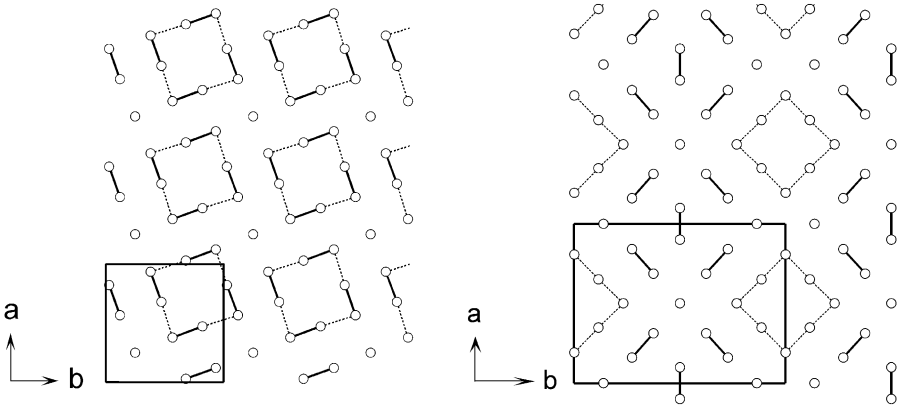

Fig. 5. Projection of the Se-deficient [Se]-sheets of $NdSe_{1.9}$ ($CeSe_{1.9}$ type, left) and Gd_8Se_{15} (right).

contained single anions, dimers and pairs of vacancies. Some of these patterns can also be observed in $Nd_{0.6}Gd_{0.4}Se_{1.85}$. In addition, the authors clearly ruled out the occurrence of higher Se oligomers, like, e.g., Se_3^{4-}.

The modulation of the *Ln* atoms is much more pronounced along *c* than within the pseudo-tetragonal plane and is directly linked to the strong modulation in the Se square layer. The modulation of the Se(1) atoms along *c* is coupled with the modulation of the *Ln* atoms, and the *Ln*–Se(1) distances therefore only vary from 2.93 to 3.07 Å, within the range of the respective distances in the binary selenides $NdSe_{1.9}$ (2.97–3.08 Å) and Gd_8Se_{15} (2.88–3.06 Å). The *Ln*–Se(2) distances, on the other hand, vary between 2.96 and 3.26 Å, slightly more than in the binary compounds ($NdSe_{1.9}$: 3.00–3.22 Å; Gd_8Se_{15}: 2.92–3.08 Å). Fig. 6 shows the slight alteration of the *Ln*–Se(1) distances (left) and the larger ones for the *Ln*–Se(2) distances (right) along the first modulation direction $t1$, which is the internal coordinate corresponding to q_1' (cf. Ref. [14], for a definition of t). Fig. 7 shows the range of the Se(2)–Se(2) distances from which the much larger variations are visible.

4. Conclusion

The modulated structure of $Nd_{0.6}Gd_{0.4}Se_{1.85}$ has been solved using the superspace approach. It can be described based on a ZrSSi like arrangement with [*Ln*Se] double slabs and planar [Se] layers. The origin of the modulation is a site occupancy wave coupled to a charge density wave in the planar selenium layer of the compound. As a result, vacancies, single Se^{2-} anions, and Se_2^{2-} dimers occur in the planar [Se] layers.[3] Several features complicate the structure solution. One is the obvious disorder, clearly visible in the diffraction pattern as diffuse scattering. The disorder mainly affects the distribution of dimers and single anions in the selenium layer and thus the interpretation of the respective interatomic distances. Secondly, the refinement of a non-harmonic behavior by a sum of harmonics is necessarily an approximation. The modulation strongly affects the occupancies of the layer

[3] We avoid this expression defective lattice charge density wave in the discussion because the disordered pattern in the [Se] layer does not match the original formulation given in Ref. [8].

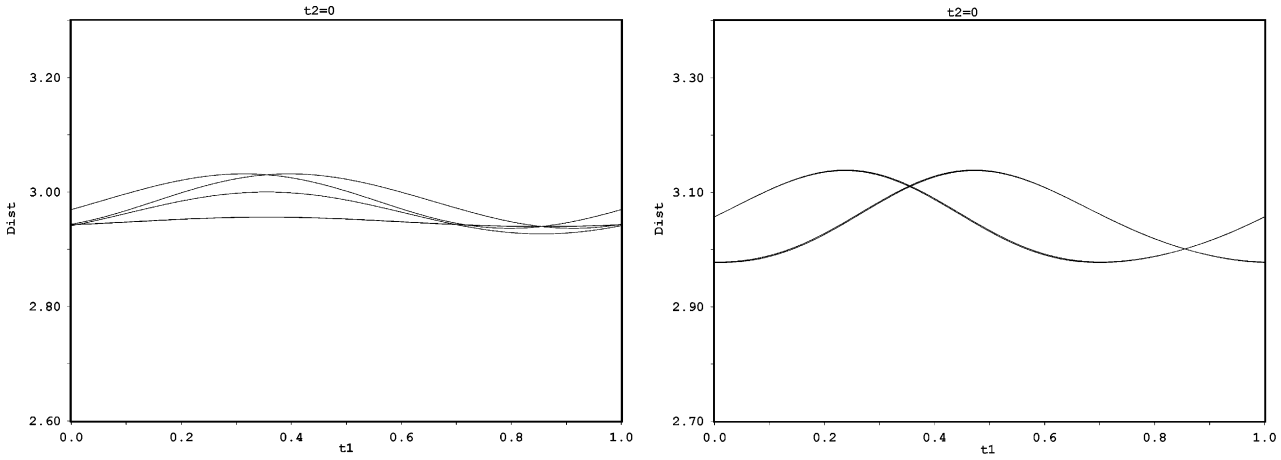

Fig. 6. Variation of the *Ln*–Se(1) distances (left) and *Ln*–Se(2) distances (left) along *t*1.

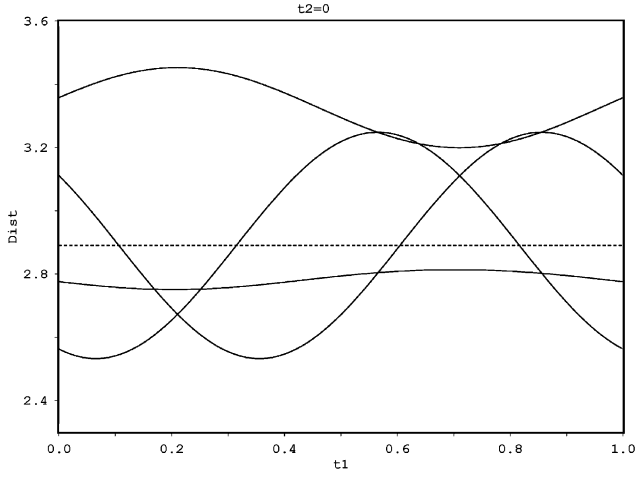

Fig. 7. Variation of the Se(2)–Se(2) distances along *t*1; (- - -) gives the respective value for a non-modulated layer.

positions and structure images therefore depend on the cutoff value chosen for the representation of the respective atoms. The true selenium content in the layer may still differ somewhat from the one depicted since several atoms have occupancies only slightly above the threshold. For these reasons, the structure images given in Fig. 4 provide an appropriate, although perhaps not completely satisfying representation of the [Se] layer in the present structure. Future investigations focusing on modeling of the atomic positions should be used to confirm the crystallographic results and to gain more insight into disordered patterns of this type.

Note added in proof

During revision of the manuscript, the crystal structure of $GdS_{1.82}$ has been published [19]. $GdS_{1.82}$ is closely related to $Nd_{0.6}Gd_{0.4}Se_{1.85}$ and the other compounds discussed above since it adopts the same basic structure. Moreover, this compound exhibits a site occupancy and a charge density wave-like modulation; its structure has been refined in the $(3+2)$-dimensional superspace group $P4/n(\alpha\beta\frac{1}{2})00ss$. The planar sulfur layer contains vacancies, single S^{2-} anions, and S_2^{2-} in a similar distribution as found in $Nd_{0.6}Gd_{0.4}Se_{1.85}$ and $DySe_{1.84}$.

Acknowledgments

The authors thank Vaclav Petricek for helpful discussions concerning the refinements of the modulated structure. TD and BPFT would like to thank the Deutsche Forschungsgemeinschaft and SL and FJGG the Swedish Science Council (Vetenskapsrådet) for financial support.

References

[1] J.A. Aitken, J.A. Cowen, M.G. Kanatzidis, Chem. Mater. 10 (1998) 3928.
[2] (a) W. Tremel, R. Hoffmann, J. Am. Chem. Soc. 109 (1987) 124;
(b) R. Hoffmann, Solids and Surfaces, VCH, New York, 1988;
(c) G.A. Papoian, R. Hoffmann, Angew. Chem. Int. Ed. 39 (2000) 2408.
[3] P. Böttcher, Th. Doert, H. Arnold, R. Tamazyan, Z. Kristallogr. 215 (2000) 246.
[4] (a) S. Benazeth, D. Carré, P. Laruelle, Acta Crystallogr. B 38 (1982) 33;
S. Benazeth, D. Carré, P. Laruelle, Acta Crystallogr. B 38 (1982) 37;
(b) J.P. Marcon, R. Pascard, C. R. Seances de l'Acad. Sci. Serie C 266 (1968) 270;
(c) P. Plambeck-Fischer, Ph.D. Thesis, Hannover, 1988.
[5] (a) P. Plambeck-Fischer, W. Abriel, W. Urland, J. Solid State Chem. 78 (1989) 164;

(b) W. Urland, P. Plambeck-Fischer, M. Grupe, Z. Naturforsch. 44b (1989) 261;
(c) M. Grupe, W. Urland, J. Less-Common Met. 170 (1991) 271;
(d) E. Dashjav, Th. Doert, P. Böttcher, Hj. Mattausch, O. Oeckler, Z. Kristallogr. NCS 215 (2000) 337.

[6] (a) M. Grupe, Ph.D. Thesis, Hannover, 1991;
(b) K. Müller, Ph.D. Thesis, Karlsruhe, 1991;
(c) K.G. Adams, Diploma Thesis, Karlsruhe, 1993;
(d) E. Dashjav, O. Oeckler, Th. Doert, Hj. Mattausch, P. Böttcher, Angew. Chem. Int. Ed. 39 (2000) 1987;
(e) E. Dashjav, Ph.D. Thesis, Dresden, 2001;
(f) B.P.T. Fokwa, Th. Doert, P. Böttcher, Z. Anorg. Allg. Chem. 628 (2002) 2167.

[7] (a) B. Foran, S. Lee, M.C. Aronson, Chem. Mater. 5 (1993) 974;
(b) S. Lee, B. Foran, J. Am. Chem. Soc. 118 (1996) 9139;
(c) A. van der Lee, L.M. Hoistad, M. Evain, B.J. Foran, S. Lee, Chem. Mater. 9 (1997) 218.

[8] S. Lee, B. Foran, J. Am. Chem. Soc. 116 (1994) 154.

[9] STOE IPDS-Software, STOE & Cie., Darmstadt, 1996.

[10] JANA2000, Crystallographic Computing System, V. Petricek, M. Dusek, Prague, 2002.

[11] X-RED: Program for data reduction and absorption correction, STOE & Cie., Darmstadt, 2001; X-SHAPE: Crystal Optimisation for Numerical Absorption Correction, STOE & Cie., Darmstadt, 1999.

[12] G. Bergerhoff, DIAMOND, Visual Crystal Information System, Bonn, 1999.

[13] (a) A.J.C. Wilson (Ed.), International Tables for Crystallography, Part C, Kluwer Academic Publishers, Dordrecht, 1995;
(b) A. Yamamoto, Acta Crystallogr. A 52 (1996) 509.

[14] JANA98 Software Manual, V. Petricek, M. Dusek, Prague, 2000, http://www-X-ray.fzu.cz/jana/jana.html.

[15] (a) R.A. Tamazyan, V.N. Molchanov, G.M. Kuzmicheva, I.G. Vasil'eva, Zh. Neorg. Khim. 39 (1994) 41;
(b) N.V. Podberezskaya, D.Yu. Naumov, I.G. Vasil'eva, N.V. Pervukhina, S.A. Magarill, S.V. Borisov, J. Struct. Chem. 39 (1998) 710;
(c) S.V. Belaya, I.G. Vasilyeva, N.V. Pervukhina, N.V. Podberezskaya, A.P. Eliseev, J. Alloys Compounds 323–324 (2001) 26.

[16] (a) P. Böttcher, Z. Anorg. Allg. Chem. 432 (1977) 167;
(b) P. Böttcher, Z. Anorg. Allg. Chem. 461 (1980) 13.

[17] (a) R. Patschke, J. Heising, J. Schindler, C.R. Kannewurf, M.G. Kanatzidis, J. Solid State Chem. 135 (1998) 111;
(b) R. Patschke, J. Heising, P. Brazis, C.R. Kannewurf, M.G. Kanatzidis, Chem. Mater. 10 (1998) 695;
(c) K.-S. Choi, R. Patschke, S.J.L. Billinge, M.J. Waner, M. Dantus, M.G. Kanatzidis, J. Am. Chem. Soc. 120 (1998) 10706;
(d) R. Patschke, P. Brazis, C.R. Kannewurf, M.G. Kanatzidis, J. Mater. Chem. 9 (1999) 2293;
(e) K. Stöwe, Z. Kristallogr. 216 (2001) 215;
(f) R. Patschke, M.G. Kanatzidis, Phys. Chem. Chem. Phys. 4 (2002) 3266.

[18] (a) D.G. Pettifor, R. Podloucky, Phys. Rev. Lett. 53 (1984) 1080;
(b) J.K. Burdett, S. Lee, J. Am. Chem. Soc. 107 (1985) 3063;
(c) S. Lee, B.J. Foran, J. Am. Chem. Soc. 116 (1994) 154.

[19] R. Tamazyan, S.v. Smaalen, I.G. Vasilyeva, H. Arnold, Acta Crystallogr. B 59 (2003) 709.